Hybrid nanostructures consisting of as-grown graphene and copper nanoparticles have been developed to improve the intensity and stability of surface plasmon resonance

Kubura Motalo [1], Lolade Nojeem [1], Joe Ewani [2], Atora Opuiyo [2], Ibrina Browndi [2]
[1] Department of Computer Science, Rivers State University, Port Harcourt, Nigeria
[2] Department of Urban and Regional Planning, Rivers State University, Port Harcourt, Nigeria

ABSTRACT

The transfer-free fabrication of the high quality graphene on the metallic nanostructures, which is highly desirable for device applications, remains a challenge. Here, we develop the transfer-free method by direct chemical vapor deposition of the graphene layers on copper (Cu) nanoparticles (NPs) to realize the hybrid nanostructures. The graphene as-grown on the Cu NPs permits full electric contact and strong interactions, which results in a strong localization of the eld at the graphene/copper interface. An enhanced intensity of the localized surface plasmon resonances (LSPRs) supported by the hybrid nanostructures can be obtained, which induces a much enhanced unresent intensity from the dye coated hybrid nanostructures. Moreover, the graphene sheets covering completely and uniformly on the Cu NPs act as a passivation layer to protect the underlying metal surface from air oxidation. As a result, the stability of the LSPRs for the hybrid nanostructures is much enhanced compared to that of the bare Cu NPs. The transfer-free hybrid nanostructures with enhanced intensity and stability of the LSPRs will enable their much broader applications in photonics and optoelectronics.

KEYWORDS: large-eddy simulation, superhydrophilicity, drag reduction, quantum system

1.0 INTRODUCTION

Graphene as two-dimensional one-atom-thick sheet of carbon has shown its potential for a wide variety of applications. Recently, hybrid nanostructures consisting of graphene and metallic nanostructures have attracted much attention because of the enhanced light–matter interactions in the hybrid nanostructures, which hold great promise for applications in photonics and optoelectronics. Metallic nanoparticles (NPs) have shown prominent optical properties due to localized surface plasmon resonances (LSPRs) associated with the excita- tion of a collective oscillation of electrons. An enhanced intensity of the LSPRs induced by the enhanced light–matter interactions is expectable for the hybrid nanostructures of graphene/metal NPs. Copper (Cu) has competitive advantages over the noble metals in low cost, compatibility of integrated circuit, high thermal and electrical conductivities and low electro-migration resistance [1-13]. However, the Cu NPs are chemically reactive and rapidly oxidized under ambient conditions, which results in degradation in the LSPRs intensity. Protective coatings are usually applied to guard the Cu NPs against reactive environments, while the protec- tive coating-induced changes of the optical or electrical properties of the Cu surface should be avoided. Graphene can act as an optically thin oxidation barrier to a pure unoxidized metal surface with minimized changes to the physical properties of the protected Cu. us, simultaneous improvement in both intensity and stability of the LSPRs supported by the Cu NPs is expectable by coating graphene onto the Cu NPs to form the graphene/Cu NPs hybrid nanostructures. The graphene/metal hybrid nanostructures are usually fabricated by separate preparation of metal nanostruc- tures and wet etching and transferring the CVD grown graphene onto the metal nanostructures. However, the etching and transferring processes generate structural and chemical deterioration in the graphene thin lm. It is time-consuming and inevitably requires the disposal of the metal substrates, generating hazardous chemical waste, which signicantly limits the cost-competitive and environmentally friendly mass production of graphene-based devices. Moreover, the incomplete contact between the graphene and metal surface impedes the graphene-induced light–matter interactions. Additionally, Cu-based nanostructures are not suitable for this method since they would be etched by the ferric chloride corrosion liquid during the transferring process. So far, the transfer-free fabrication of the high quality graphene/Cu NPs hybrid nanostructures remains a challenge [14-27].

Here, we develop an etching and transfer-free technique for one-step fabrication of the graphene/Cu NPs hybrid nanostructures by direct growth of graphene on the hemispherical copper nanoparticles to form graphene-coated hemispheres with Cu cores. e as-grown graphene/Cu NPs hybrid nanostructures exhibit enhancements in both intensity and stability of the LSPRs due to the graphene-induced enhancement in the light–matter interactions and the surface passivation. e as-grown graphene on the Cu NPs is biennial to their full electric contact and strong interactions on account of the larger adhesion energy. 10-fold enhancement of putrescence from the dye coated hybrid nanostructures has been obtained due to graphene-induced enhanced LSPRs, which has been supported by nitedierence time domain (FDTD) calculation. Moreover, the stability of the LSPRs for the hybrid nanostructures is much enhanced compared to that of the bare Cu NPs due to the surface passivation of the graphene sheets covering completely and uniformly on the Cu NPs. Our dings might open up a new avenue to realize high quality graphene/Cu NPs hybrid nanostructures and ful l their practical applications in photonics and optoelectronics [28-35].

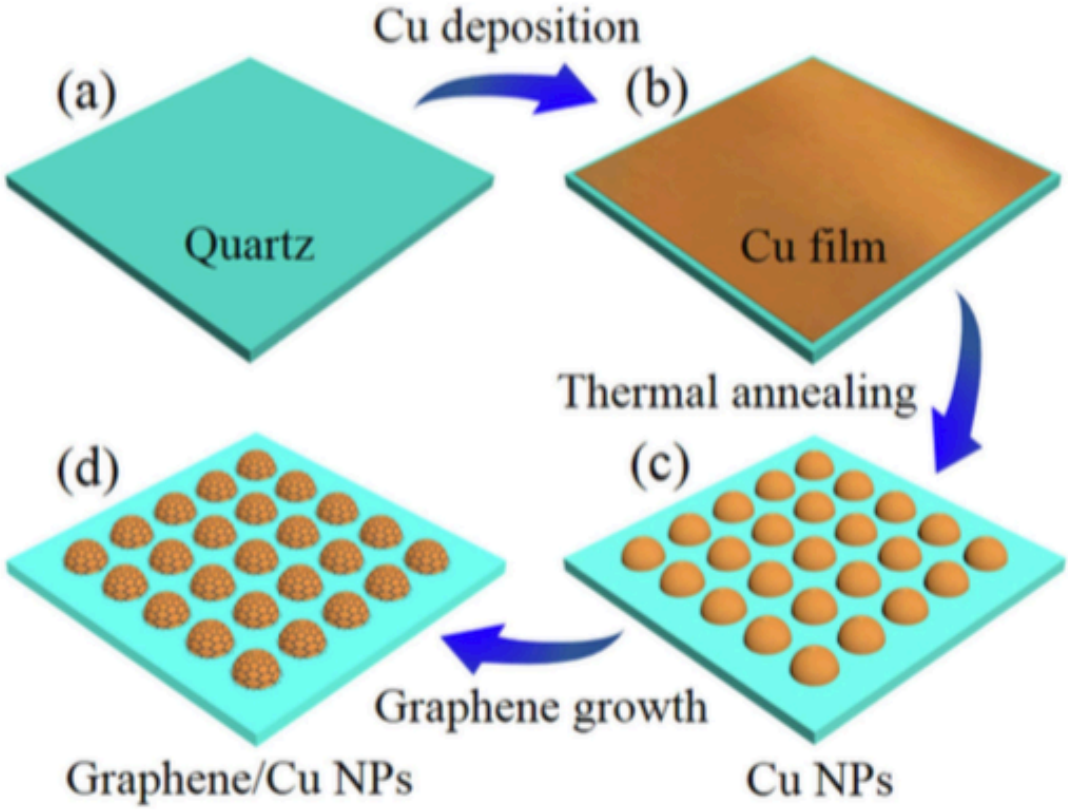

Figure 1. Schematic illustrations of fabrication sequences for the as-grown graphene/Cu NPs hybrid nanostructures. (**a**,**b**) Deposition of the Cu lm on the quartz substrate. (**c**) ermal annealing of the Cu lm. (**d**) Deposition of the graphene on the Cu NPs.

2.0 RESEARCH METHODOLOGY

Fabrication and characterization of graphene/Cu NPs hybrid nanostructures: e copper lms of 40 nm were fabricated on the pre-cleaned quartz substrates (cleaned by acetone, ethanol and ultrapure water, respectively) via thermal evaporation with pieces of copper foil (Alfa Aesar, item No. 46356) at a base pressure of 5 × 10−4 Pa. ermal annealing then preformed in the low pressure chemical vapor deposition (LPCVD) system at the atmosphere of hydrogen (H2) and argon (Ar) gas to obtain copper nanoparticles with morphology-controllable characteristics. A er the introduction of methane (CH4) gas into the chamber at the proper temperature of 1000 °C, graphene/copper nanoparticles hybrid nanostructures can be realized directly a er the rapid cooling without time-consuming transfer method.

e gas ow rates of CH4, H2 and Ar were 7, 30, 200 standard cubic centimeters per minute (sccm), respectively [1-17]. e ramping rate of the temperature was approximately 40 °C/min, followed by rapid cooling to room temperature (25 °C) with protective gas conguration of H2 and Ar. Scanning electron microscopy (SEM, JEOL JSM-6700F, Japan) and high resolution transmission electron microscopy (HRTEM, JEOL JEM-2100F, Japan) were utilized to measure the surface morphologies of the samples. Raman spectra (LabRAM HR Evolution Raman Spectrometer, HORIBA Scienti c, France) were obtained with a 532 nm laser to analyze the quality of graphene. In order to remove the in uence of Cu uorescence peaks overlapping with typical graphene peaks, the specimens were thoroughly soaked in 20% HNO3 for 10 h and rinsed in deionized water for 20 min subsequently to etch the Cu cores prior to the micro-Raman spectroscopy analysis. Absorption spectra were measured using UV-vis spectrophotometer (UV-2550, Shimadzu, Japan). e chemical composition of the specimens was characterized by X-ray photoelectron spectroscopy (XPS, ESCAL-AB250, VG Microtech, UK). A 25 nm thick emitting layer of 4-(Dicyanomethylene)-2-methyl-6-(4-dimethylaminostyryl)-4H-pyran (DCM) was thermal evaporated on the specimens of graphene lms, bare Cu NPs, graphene/Cu NPs and quartz substrates at a base pressure of 5 × 10−4 Pa. e uorescence spectra were obtained at the excitation light of 480 nm from uorescence spectrophotometer (F-4600, HITACHI, Japan) [38-48].

3.0 RESULT

The specic fabrication procedures of the as-grown graphene on the hemispherical copper nanoparticles are schematically summarized in Fig. 1 and illustrated in the experimental details. During the annealing process of high temperature, copper lm melts into nanoparticles and patterned graphene lms directly form on them without transfer method. e surface morphologies of the copper nanoparticles coated with and without the as-grown graphene layers are investigated by scanning electron microscopy (SEM) and high resolution transmission electron microscopy (HRTEM) and shown in Fig. 2a,b, respectively. ere is no apparent morphological variation except irregular edges with the as-grown graphene. e Cu NPs with diverse size distributions mainly ranges from 600 to 800 nm (Fig. 2c,d).

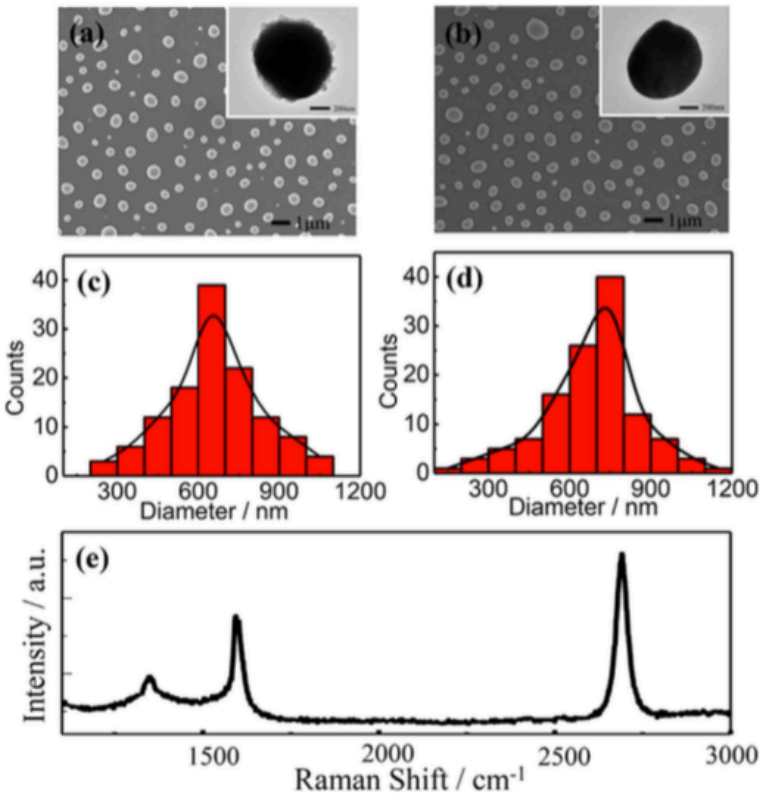

Figure 2. (**a**,**b**) SEM images and HRTEM images (the inset gures) of Cu NPs with and without graphene as protective layers, respectively. (**c**,**d**) Size distributions of as-grown graphene/Cu NPs hybrid nanostructures and

bare Cu NPs. (**e**) Normal Raman spectrum of graphene a er removing Cu cores.

It has been demonstrated that the graphene encapsulation process performed on the separately prepared Cu NPs is prone to induce agglomeration at high temperature when gas carbon source such as methane or ethylene is supplied for the growth of graphene29,41. While in our case, the Cu NPs are not agglomerated during the annealing process at high temperature of 1000 °C even using methane as gas carbon source in this one-step method. is can probably be attributed to the synchronous synthesis of Cu NPs and graphene layers, where Cu NPs could be defended against morphological destruction by the as-grown protective graphene shells during the annealing procedure. To further con rm the formation and investigate the quality of graphene layers coated on the Cu NPs, we conduct typical Raman measurements using laser wavelength of 532 nm as shown in Fig. 2e. ree most intensive features associated with graphene, the D peak at 1337 cm−1, the G peak at 1580 cm−1 and the 2D peak at 2659 cm−1 are observed, respectively, which con rms the direct synthesis of few layer graphene on Cu NPs. In particular, the D peak at 1337 cm−1 originates in the lattice disorder probably arising from the etch process for analysis or the high curvature of Cu NPs surfaces, rather than the practical defects in the graphitic lattice.

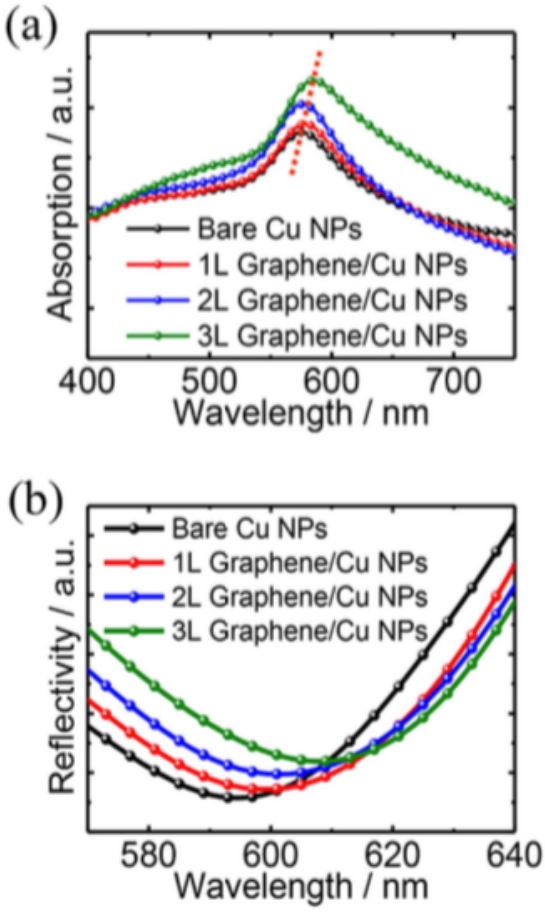

Figure 3. (a) Steady-state optical absorption spectra versus wavelength for the Cu NPs coated with various numbers of graphene layers. (b) Simulated re ection spectra of Cu NPs coated with various numbers of graphene layers.

To shed light on the speci c function of graphene coupling to the LSPRs of the metal nanoparticles, the steady-state optical absorption spectra for the Cu NPs with or without the graphene coating are compared and shown in Fig. 3a. e layer numbers of graphene can be precisely controlled from single layer to three layers by adjusting the gas concentration and growth time. e enhanced absorption intensity can be observed with the increased layer numbers of the graphene, meanwhile, the absorption

peaks redshi gradually. e presence of the graphene sheets results in a strong localization of the eld at the graphene/Cu NPs interface and a drastic eld enhancement, especially with full electric contact and strong interactions in the hybrid nanostructures. It has been reported that electrons would transfer from graphene to the surface of Cu thin lm in order to maintain the continuity of the Fermi levels when they contact with each other, as the work function of Cu (5.22 eV) is larger than that of graphene (4.5 eV). Therefore, charge transfer is one of the main reasons for the LSPRs enhancement induced by the graphene layers. Besides, the as-grown graphene on the Cu NPs is beneficial to their full electric contact and strong interactions arising from the larger adhesion energy, since the attractive intersurface forces such as van der Waals pull the graphene sheets into tight contact with the growth substrate, where an enhanced intensity of the LSPRs supported by the hybrid nanostructures can be obtained. e LSPRs are highly sensitive to the surrounding environment where graphene acts as a lossy dielectric with higher refractive index in the visible and near-infrared wavelength, which results in the redshift of the LSPRs wavelength with the increased layer number of the graphene.

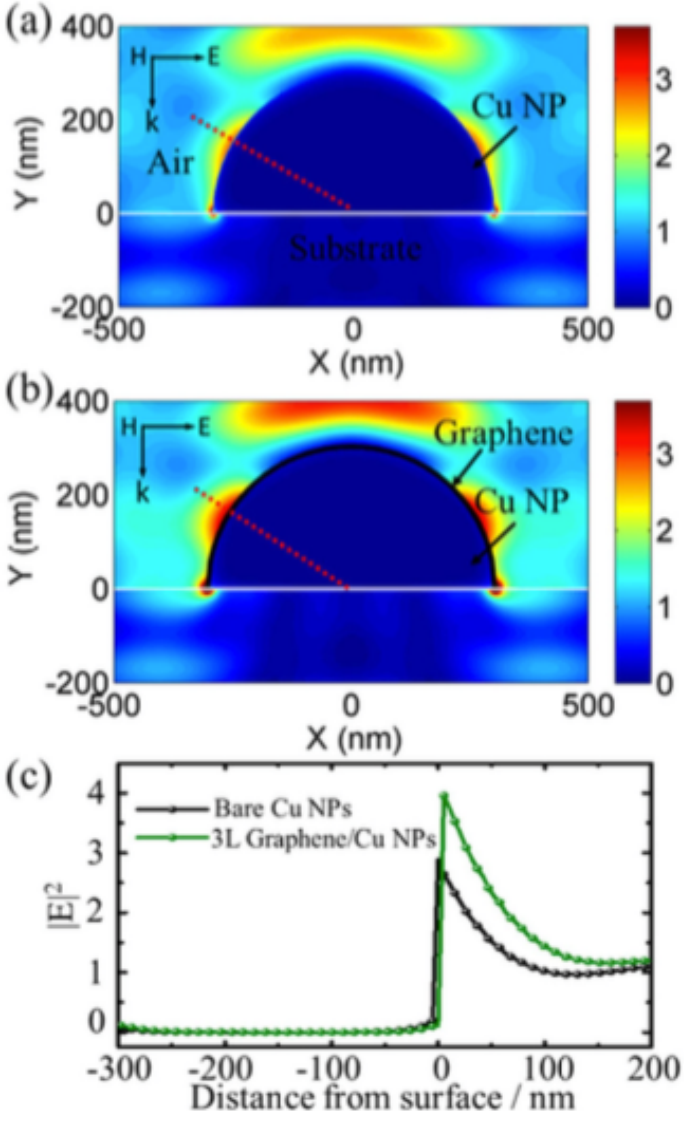

Figure 4. Simulated electrical eld distributions for the bare Cu NP (a) and as-grown graphene/Cu NP hybrid nanostructure (b). (c) Cross-section plots for total electric elds of Cu NP along the red dot line in (a,b) with (green) and without (black) graphene layer, respectively.

In-house-generated finite-difference time-domain (FDTD) simulations are performed to further investigate the LSPRs enhancement induced by the graphene coating. We calculate the reflection

spectra of the graphene-coated Cu NPs arrays versus deferent numbers of the graphene layers as shown in Fig. 3b, where the redshift and low reaction can be observed with increased graphene layer numbers. It is noteworthy that we treat monolayer graphene as an effective medium with thickness of 1 nm which is reasonable for CVD-grown graphene. is shows a good agreement with the experimental results and indicates that the strong light-graphene interactions can account for the remarkable resonance shi as well as enhanced absorption between 400 nm and 750 nm44. More specifically, the redfish of the resonance is a result of the introduction of the graphene layers, since besides the metal properties, the LSPRs are also determined by the refractive index of the environment. e broadband absorption enhancement is due to the fact that graphene is a good absorber in optical frequency region. Figure 4a,b illustrate the normalized electrical eld distributions for the corresponding LSPRs excited in the bare Cu NP and graphene/Cu NP hybrid nanostructure with the incident light at the wavelength of 595 nm and 610 nm, respectively. e eld intensity |E|2 exhibits its maximum at the surface of Cu NPs and shows exponential decay along the direction perpendicular to it, demonstrating the excitation of the LSPRs. In this case, the presence of graphene sheets leads to a strong localization of the eld at the graphene–copper interface, as shown in Fig. 4b, when compared with the bare Cu NPs in Fig. 4a. e cross-section plots for total electric elds (Fig. 4c) indicate the obvious eld enhancement for the hybrid nanostructures. LSPRs have e ect on uores- cence enhancement for the uorescent dye adsorbed on the metallic NPs through the strong coupling between the dye molecule resonance and the NPs LSPRs. Fluorescence spectra of the 4-(Dicyanomethylene)-2-methyl- 6-(4-dimethylaminostyryl)-4H-pyran (DCM) dye deposited on the as-grown graphene/Cu NPs hybrid nano- structures, bare Cu NPs and graphene lms, respectively, are measured and compared to examine the LSPRs enhancement. As can be seen in Fig. 5, a highest uorescence enhancement factor of 10.0 is obtained from the hybrid nanostructures with three-layered graphene compared to the DCM on bare quartz substrate, while the enhancement factors are 4.0 and 1.7, respectively, for that on the Cu NPs and graphene lms. e highest uores- cence enhancement should be attributed to the enhanced intensity of the LSPRs supported on the graphene/Cu NPs hybrid nanostructures.

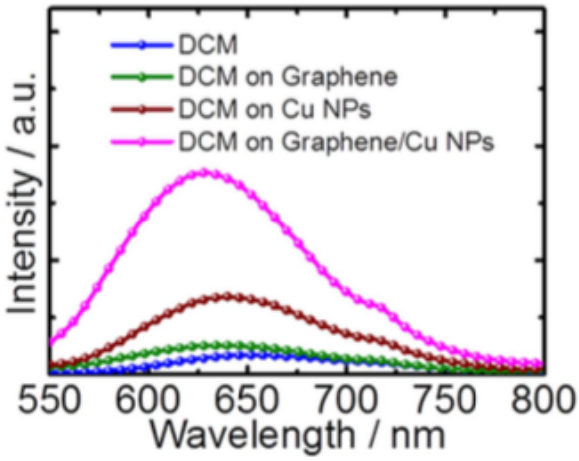

Figure 5. Fluorescence spectra of DCM dye on quartz substrate, graphene lms, bare Cu NPs, and as- grown graphene/Cu NPs hybrid nanostructures, respectively.

The surface of the bare copper is prone to proceed oxidation as exposed to the ambient air, leading to the development of layers consisting of cuprous oxide (Cu2O), cupric oxide (CuO) and copper hydroxide (Cu(OH)2)19,20,23,46. In order to evaluate the passivation of the graphene on the Cu NPs, the UV–Vis absorption spectra during the time of exposure to ambient air for Cu NPs with or without the coating of three-layered graphene are investigated and shown in Fig. 6. For the fresh Cu NPs with or without the graphene coating, their absorption spectra show a prominent absorption peak at around 580 nm. Red-shi and degradation of the LSPRs can be observed for both bare and graphene-coated Cu NPs with the increased exposure time. However, the degradations are much smaller for the hybrid nanostructures. Especially, the absorption peak of the bare Cu NPs almost disappears a er 7 days exposure, which indicates the complete oxidation of the bare Cu NPs due to their active property. While in case of the hybrid nanostructures, the much improved stability of the LSPRs veri es the e ective passivation of the graphene.

To further evaluate the graphene passivation, X-ray photoelectron spectroscopy (XPS) measurement is carried out to analyze the metal composition. Figure 7a shows the XPS spectra of bare Cu NPs and three-layered- graphene/Cu NPs hybrid nanostructures before and a er thermal treatment at 200 °C for 4 hours in ambient conditions. Several studies have proposed that the surface oxidation for polycrystalline Cu proceeds in four distinct steps: (a) dissociative adsorption of O2, (b) initial formation of cuprous oxide (Cu2O), (c) formation of cupric oxide (CuO) islands, and (d) further formation of copper hydroxide (Cu(OH)2)20. Here, the XPS spectra of graphene coated Cu NPs (Fig. 7a, le) exhibit two prominent Cu peaks representing Cu 2p3/2 and Cu 2p1/2 at binding energies of 932.2 eV, 952.3 eV (before thermal treatment) and 932.8 eV, 952.5 eV (a er thermal treat- ment), respectively, which indicates negligible oxidation of the graphene/Cu NPs hybrid nanostructures a er thermal treatment. However, in case of the bare Cu NPs (Fig. 7b, right), broader peaks corresponding to di erent copper oxides composition, Cu2O (932.7 and 952.3 eV), CuO (933.7 and 953.4 eV), and Cu(OH)2 (935.1 and 954.5 eV) are formed a er thermal treatment for 4 hours. e photograph images of both thermal treatments are shown in Fig. 7b. e graphene/Cu NPs hybrid nanostructures exhibit little visible variations, in contrast with the bare Cu NPs whose surface morphology changes remarkably. e XPS datas and photograph images combined with the absorption spectra demonstrate that the graphene coating is e ective on protecting the underlying Cu NPs from oxidation.

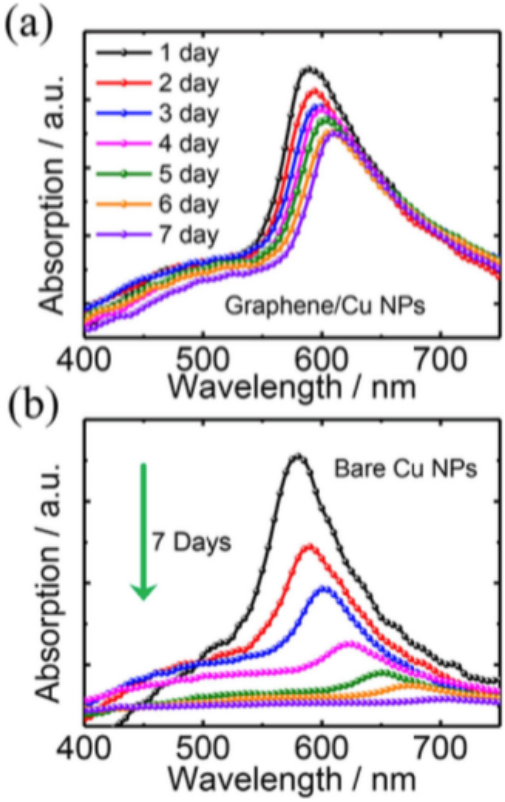

Figure 6. Time evolution of the absorption spectra of graphene-coated (a) and uncoated (b) Cu NPs.

binding energies of 932.2 eV, 952.3 eV (before thermal treatment) and 932.8 eV, 952.5 eV (a er thermal treat- ment), respectively, which indicates negligible oxidation of the graphene/Cu NPs hybrid nanostructures a er thermal treatment. However, in case of the bare Cu NPs (Fig. 7b, right), broader peaks corresponding to di erent copper oxides composition, Cu2O (932.7 and 952.3 eV), CuO (933.7 and 953.4 eV), and Cu(OH)2 (935.1 and 954.5 eV) are formed a er thermal treatment for 4 hours. e photograph images of both thermal treatments are shown in Fig. 7b. e graphene/Cu NPs hybrid nanostructures exhibit little visible variations, in contrast with the bare Cu NPs whose surface morphology changes remarkably. e XPS datas and photograph images combined with the absorption spectra demonstrate that the graphene coating is e ective on protecting the underlying Cu NPs from oxidation.

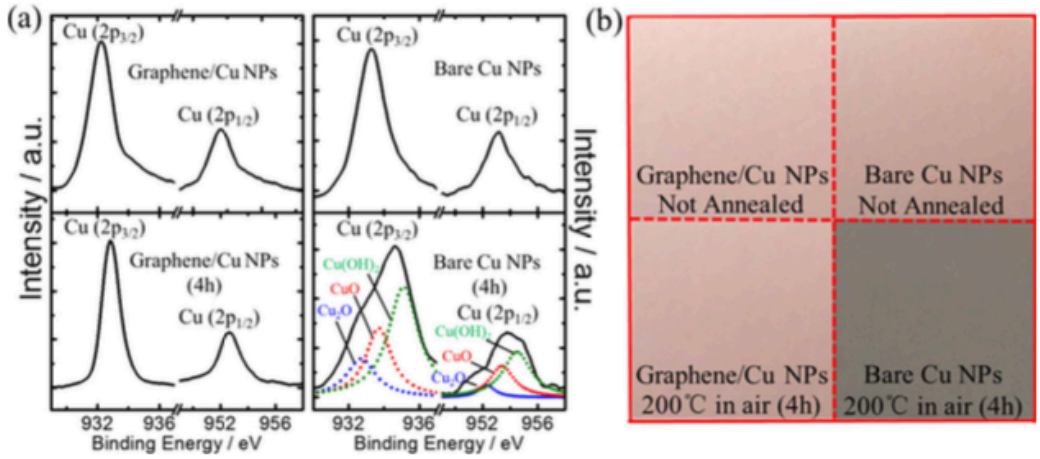

Figure 7. Time evolution of the XPS core-level Cu2p spectra (**a**) and photograph images (**b**) of graphene/Cu NPs hybrid nanostructures and bare Cu NPs before and after thermal treatment at 200 °C for 4 hours.

4.0 CONCLUSION

The goal of the study was to enhance the intensity and stability of surface plasmon resonance using hybrid nanostructures of as-grown graphene and copper nanoparticles. The researchers investigated the properties of these hybrid structures and compared them to those of bare copper nanoparticles. The results demonstrated that the graphene/copper nanoparticles hybrid structures exhibit a stronger and more stable surface plasmon resonance signal, indicating their potential for improving the performance of plasmonic devices. The findings suggest that the incorporation of graphene in plasmonic devices can enhance their properties and contribute to the development of new applications in various fields. Fabrication and characterization of graphene/Cu NPs hybrid nanostructures: e copper lms of 40 nm were fabricated on the pre-cleaned quartz substrates (cleaned by acetone, ethanol and ultrapure water, respectively) via thermal evaporation with pieces of copper foil (Alfa Aesar, item No. 46356) at a base pressure of 5 × 10−4 Pa. ermal annealing then preformed in the low pressure chemical vapor deposition (LPCVD) system at the atmos- phere of hydrogen (H2) and argon (Ar) gas to obtain copper nanoparticles with morphology-controllable char- acteristics. A er the introduction of methane (CH4) gas into the chamber at the proper temperature of 1000 °C, graphene/copper nanoparticles hybrid nanostructures can be realized directly a er the rapid cooling without time-consuming transfer method. e gas ow rates of CH4, H2 and Ar were 7, 30, 200 standard cubic centimeters per minute (sccm), respectively. e ramping rate of the temperature was approximately 40 °C/min, followed by rapid cooling to room temperature (25 °C) with protective gas con guration of H2 and Ar. Scanning electron microscopy (SEM, JEOL JSM-6700F, Japan) and high resolution transmission electron microscopy (HRTEM, JEOL JEM-2100F, Japan) were utilized to measure the surface morphologies of the samples. Raman spectra (LabRAM HR Evolution Raman Spectrometer, HORIBA Scienti c, France) were obtained with a 532 nm laser to analyze the quality of graphene. In order to remove the in uence of Cu uorescence peaks overlapping with typical graphene peaks, the specimens were thoroughly soaked in 20% HNO3 for 10 h and rinsed in deionized water for 20 min subsequently to etch the Cu cores prior to the micro-Raman spectroscopy analysis. Absorption spectra were measured using UV-vis spectrophotometer (UV-2550, Shimadzu, Japan). e chemical composition of the specimens was characterized by X-ray photoelectron spectroscopy (XPS, ESCAL-AB250, VG Microtech, UK). A 25 nm thick emitting layer of 4-(Dicyanomethylene)-2-methyl-6-(4-dimethylaminostyryl)-4H-pyran (DCM) was thermal evaporated on the specimens of graphene lms, bare Cu NPs, graphene/Cu NPs and quartz substrates at a base pressure of 5 × 10−4 Pa. e uorescence spectra were obtained at the excitation light of 480 nm from uorescence spectrophotometer (F-4600, HITACHI, Japan). In conclusion, we have demonstrated a novel and facile route to fabricate the hybrid nanostructures of as-grown etching-free graphene on Cu NPs with full electric contact and strong interactions by the chemical vapor depo- sition (CVD) process. Few-layer graphene can be directly synthesized on the Cu NPs, which is veri ed from the Raman spectroscopy and HRTEM micrographs. e intensity of the LSPRs supported by the graphene/Cu NPs hybrid nanostructures has been improved, and results in an 10-fold enhanced uorescent intensity from the dye coated hybrid nanostructures. e stability of the

LSPRs for the hybrid nanostructures has been much enhanced compared to that of the bare Cu NPs due to the passivation of the graphene coating. e transfer-free hybrid nanostructures with enhanced intensity and stability of the LSPRs might play a signi cantly important role in the development of Cu-based plasmonic nanostructures, hybrid nanophotonic and optoelectronic devices and ultra-large-scale integrated circuits.

REFERENCES

[1] Tian, Wei, et al. "Hybrid nanostructures for photodetectors." Advanced Optical Materials 5.4 (2017): 1600468.
[2] Tang, Zuge, Behrad Zeinali, and Sarkew S. Abdulkareem. "Phase controlling of electromagnetically induced grating." Laser Physics Letters 19.5 (2022): 055204.
[3] Huang, Xiao, et al. "25th Anniversary article: hybrid nanostructures based on two-dimensional nanomaterials." Advanced Materials 26.14 (2014): 2185-2204.
[4] Zare, Saman, Behrad Zeinali Tajani, and Sheila Edalatpour. "Effect of nonlocal electrical conductivity on near-field radiative heat transfer between graphene sheets." Physical Review B 105.12 (2022): 125416.
[5] Yu, Taekyung, et al. "Aqueous-Phase Synthesis of Pt/CeO2 Hybrid Nanostructures and Their Catalytic Properties." Advanced Materials 22.45 (2010): 5188-5192.
[6] Afroozeh, Abdolkarim, and Behrad Zeinali. "Improving the sensitivity of new passive optical fiber ring sensor based on meta-dielectric materials." Optical Fiber Technology 68 (2022): 102797.
[7] Xiao, Fang-Xing, et al. "One-dimensional hybrid nanostructures for heterogeneous photocatalysis and photoelectrocatalysis." Small 11.18 (2015): 2115-2131.
[8] Zeinali, Behrad, and Jafar Ghazanfarian. "Turbulent flow over partially superhydrophobic underwater structures: The case of flow over sphere and step." Ocean Engineering 195 (2020): 106688.
[9] Camargo, Pedro HC, et al. "Facile synthesis of tadpole-like nanostructures consisting of Au heads and Pd tails." Journal of the American Chemical Society 129.50 (2007): 15452-15453.
[10] Zeinali, Behrad, Jafar Ghazanfarian, and Bamdad Lessani. "Janus surface concept for three-dimensional turbulent flows." Computers & Fluids 170 (2018): 213-221.
[11] Liu, Hai, et al. "Self-organization of a hybrid nanostructure consisting of a nanoneedle and nanodot." Small (Weinheim an der Bergstrasse, Germany) 8.18 (2012): 2807-2811.
[12] Zavareh, Bozorgasl, Hossein Foroozan, Meysam Gheisarnejad, and Mohammad-Hassan Khooban. "New trends on digital twin-based blockchain technology in zero-emission ship applications." Naval Engineers Journal 133, no. 3 (2021): 115-135.
[13] Weng, Lin, et al. "Hierarchical synthesis of non-centrosymmetric hybrid nanostructures and enabled plasmon-driven photocatalysis." Nature communications 5.1 (2014): 4792.
[14] Bozorgasl, Zavareh, and Mohammad J. Dehghani. "2-D DOA estimation in wireless location system via sparse representation." In 2014 4th International Conference on Computer and Knowledge Engineering (ICCKE), pp. 86-89. IEEE, 2014.
[15] Liu, Hailong, et al. "Multispectral plasmon-induced transparency in triangle and nanorod (s) hybrid nanostructures." Optics letters 38.6 (2013): 977-979.
[16] Piomelli, Ugo. "Large-eddy simulation: achievements and challenges." Progress in aerospace sciences 35.4 (1999): 335-362.
[17] Ruan, Gang, et al. "Simultaneous magnetic manipulation and fluorescent tracking of multiple individual hybrid nanostructures." Nano letters 10.6 (2010): 2220-2224.
[18] Sagaut, Pierre. Large eddy simulation for incompressible flows: an introduction. Springer Science & Business Media, 2006.
[19] Jung, Dae Soo, et al. "Pattern formation of metal–oxide hybrid nanostructures via the self-assembly of di-block copolymer blends." Nanoscale 11.40 (2019): 18559-18567.
[20] Zhiyin, Yang. "Large-eddy simulation: Past, present and the future." Chinese journal of Aeronautics 28.1 (2015): 11-24.
[21] Ran, Qiwen, et al. "Multifunctional integration of double-shell hybrid nanostructure for alleviating surface degradation of LiNi0. 8Co0. 1Mn0. 1O2 cathode for advanced lithium-ion batteries at high cutoff voltage." ACS Applied Materials & Interfaces 12.8 (2020): 9268-9276.
[22] Mason, Paul J. "Large-eddy simulation: A critical review of the technique." Quarterly Journal of the Royal Meteorological Society 120.515 (1994): 1-26.
[23] Son, Giyeong, et al. "Thioflavin T-Amyloid Hybrid Nanostructure for Biocatalytic Photosynthesis." Small 14.40 (2018): 1801396.
[24] Lesieur, Marcel, Olivier Métais, and Pierre Comte. Large-eddy simulations of turbulence. Cambridge university press, 2005.
[25] Hou, Xinghui, et al. "Hierarchical three-dimensional MoS2/GO hybrid nanostructures for triethylamine-sensing applications with high sensitivity and selectivity." Sensors and Actuators B: Chemical 317 (2020): 128236.
[26] Zalnejad, Kaveh, Seyyed Fazlollah Hossein, and Yousef Alipour. "The Impact of Livable City's Principles

on Improving Satisfaction Level of Citizens; Case Study: District 4 of Region 4 of Tehran Municipality." Armanshahr Architecture & Urban Development 12.28 (2019): 171-183.
[27] Zalnezhad, Kaveh, Mahnaz Esteghamati, and Seyed Fazlollah Hoseini. "Examining the Role of Renovation in Reducing Crime and Increasing the Safety of Urban Decline Areas, Case Study: Tehran's 5th District." Armanshahr Architecture & Urban Development 9.16 (2016): 181-192.
[28] Yun, Chidi, et al. "The use of bilayers consisting of graphene and noble metals has been explored for biosensors that employ inverted surface plasmon resonance." International Journal of Science and Information System 12.8 (2022): 441-449.
[29] Olutola, Tomiloba, et al. "A diffraction grating made of liquid crystals that can be controlled through electro-optic resources." International Journal of Management System and Applied Science 14.12 (2022): 42-51.
[30] Balen, John, et al. "Quantum plasmonic sensing is employed to experimentally measure kinetic parameters." Journal of Basis Applied Science and Management System 8.7 (2022): 136-146.
[31] Sharifani, Koosha and Amini, Mahyar and Akbari, Yaser and Aghajanzadeh Godarzi, Javad. "Operating Machine Learning across Natural Language Processing Techniques for Improvement of Fabricated News Model." International Journal of Science and Information System Research 12.9 (2022): 20-44.
[32] Amini, Mahyar, et al. "MAHAMGOSTAR.COM AS A CASE STUDY FOR ADOPTION OF LARAVEL FRAMEWORK AS THE BEST PROGRAMMING TOOLS FOR PHP BASED WEB DEVELOPMENT FOR SMALL AND MEDIUM ENTERPRISES." Journal of Innovation & Knowledge, ISSN (2021): 100-110.
[33] Amini, Mahyar, and Aryati Bakri. "Cloud computing adoption by SMEs in the Malaysia: A multi-perspective framework based on DOI theory and TOE framework." Journal of Information Technology & Information Systems Research (JITISR) 9.2 (2015): 121-135.
[34] Amini, Mahyar, and Nazli Sadat Safavi. "A Dynamic SLA Aware Heuristic Solution For IaaS Cloud Placement Problem Without Migration." International Journal of Computer Science and Information Technologies 6.11 (2014): 25-30.
[35] Amini, Mahyar. "The factors that influence on adoption of cloud computing for small and medium enterprises." (2014).
[36] Amini, Mahyar, et al. "Development of an instrument for assessing the impact of environmental context on adoption of cloud computing for small and medium enterprises." Australian Journal of Basic and Applied Sciences (AJBAS) 8.10 (2014): 129-135.
[37] Amini, Mahyar, et al. "The role of top manager behaviours on adoption of cloud computing for small and medium enterprises." Australian Journal of Basic and Applied Sciences (AJBAS) 8.1 (2014): 490-498.
[38] Amini, Mahyar, and Nazli Sadat Safavi. "A Dynamic SLA Aware Solution For IaaS Cloud Placement Problem Using Simulated Annealing." International Journal of Computer Science and Information Technologies 6.11 (2014): 52-57.
[39] Sadat Safavi, Nazli, Nor Hidayati Zakaria, and Mahyar Amini. "The risk analysis of system selection and business process re-engineering towards the success of enterprise resource planning project for small and medium enterprise." World Applied Sciences Journal (WASJ) 31.9 (2014): 1669-1676.
[40] Sadat Safavi, Nazli, Mahyar Amini, and Seyyed AmirAli Javadinia. "The determinant of adoption of enterprise resource planning for small and medium enterprises in Iran." International Journal of Advanced Research in IT and Engineering (IJARIE) 3.1 (2014): 1-8.
[41] Sadat Safavi, Nazli, et al. "An effective model for evaluating organizational risk and cost in ERP implementation by SME." IOSR Journal of Business and Management (IOSR-JBM) 10.6 (2013): 70-75.
[42] Safavi, Nazli Sadat, et al. "An effective model for evaluating organizational risk and cost in ERP implementation by SME." IOSR Journal of Business and Management (IOSR-JBM) 10.6 (2013): 61-66.
[43] Amini, Mahyar, and Nazli Sadat Safavi. "Critical success factors for ERP implementation." International Journal of Information Technology & Information Systems 5.15 (2013): 1-23.
[44] Amini, Mahyar, et al. "Agricultural development in IRAN base on cloud computing theory." International Journal of Engineering Research & Technology (IJERT) 2.6 (2013): 796-801.
[45] Amini, Mahyar, et al. "Types of cloud computing (public and private) that transform the organization more effectively." International Journal of Engineering Research & Technology (IJERT) 2.5 (2013): 1263-1269.
[46] Amini, Mahyar, and Nazli Sadat Safavi. "Cloud Computing Transform the Way of IT Delivers Services to the Organizations." International Journal of Innovation & Management Science Research 1.61 (2013): 1-5.
[47] Abdollahzadegan, A., Che Hussin, A. R., Moshfegh Gohary, M., & Amini, M. (2013). The organizational critical success factors for adopting cloud computing in SMEs. Journal of Information Systems Research and Innovation (JISRI), 4(1), 67-74.
[48] Khoshraftar, Alireza, et al. "Improving The CRM System In Healthcare Organization." International Journal of Computer Engineering & Sciences (IJCES) 1.2 (2011): 28-35.